DOI: 10.1002/ejic.200500665

Reduction of $[Cp^*_2Mo_2O_5]$ in Aqueous Medium: Structure and Properties of a Triangular Mixed Oxo-Hydroxo-Bridged Product, $[Cp^*_3Mo_3(\mu\text{-}O)_2(\mu\text{-}OH)_4](X)_2$ (X = CF_3CO_2 or CF_3SO_3)

Funda Demirhan,*[a] Bahar Çağatay,[a] Deniz Demir,[a] Miguel Baya,[b] Jean-Claude Daran,[b] and Rinaldo Poli*[b]

Keywords: Bridging ligands / Hydrogen bonding / Metal–metal interactions / Molybdenum / Oxo ligands

The reduction of $[Cp^*_2Mo_2O_5]$ with Zn in a MeOH/H_2O solution acidified with either CF_3COOH or CF_3SO_3H leads to the formation of the $[Cp^*_3Mo_3(\mu\text{-}O)_2(\mu\text{-}OH)_4]^{2+}$ ion as its trifluoroacetate or trifluoromethanesulfonate salt. The structure of the compound was confirmed by X-ray analyses. The anions establish hydrogen-bonding interactions with all four bridging OH groups. Density functional calculations afford bonding parameters in close agreement with the observed structure and indicate that the cluster is best described as a valence-delocalized Mo_3^{13+} species. The five metal electrons are distributed among an *a*-type (z^2) orbital, which accounts for most of the metal–metal attraction, and two essentially metal–metal nonbonding *e*-type (*xy*) orbitals with a slight Mo-(μ-O) π*-type contribution. Because of the C_2 symmetry, the latter orbitals are not degenerate. The calculations show that the unpaired electron is located in a molecular orbital with equal contribution from two Mo atoms, in agreement with the experimental observation of coupling of the unpaired electron to two Mo atoms in the isotropic EPR spectrum.

Introduction

We have recently initiated a research program aimed at developing the chemistry of high-oxidation-state organometallic compounds in water, in the spirit of "green" chemistry[1–3] and with the long term goal of exploring the catalytic and electrocatalytic potential of organometallic compounds in water.[4,5] Unlike low-valent organometallic systems, which are generally supported by water-soluble modified phosphane or cyclopentadienyl ligands,[6–8] high-oxidation-state complexes are supported by oxo ligands, which makes them soluble in water by virtue of hydrogen bonding and protonation equilibria that yield charged hydroxo and aqua complexes. Although oxo-supported high-oxidation-state organometallic complexes are now well established and have interesting catalytic properties,[9,10] their systematic investigation in water has received little attention. We further argue that the greater metal electronegativity in these higher oxidation states confers a higher degree of covalency to the metal–carbon bonds with odd-electron carbon ligands (i.e. alkyls, allyls, cyclopentadienyls, etc.), which consequently may become quite resistant toward hydrolytic decomposition. For a redox-active metal, reduction of a high-oxidation-state oxo complex should favor the generation of aqua ligands and open the way to the generation of open coordination sites for substrate activation and catalytic and electrocatalytic applications.[11]

We have so far focused our attention on the speciation[12] and electrochemical behavior[13,14] of $[Cp^*_2Mo_2O_5]$. The Cp*–Mo bond in this complex is quite hydrolytically stable and is split only quite slowly at very low pH.[15] We have obtained novel oxo-supported complexes, the nature of which seems to depend intimately on the nature of the acid used, by chemical reduction with zinc in an acidic MeOH/H_2O mixed solvent medium. For instance, with acetic acid we isolated the dinuclear Mo^{IV} complex $[Cp^*_2Mo_2(\mu\text{-}O)_2(\mu\text{-}O_2CCH_3)_2]$ (**I**),[16] whereas with CF_3COOH under the same conditions (mixed MeOH/H_2O solvent, Zn as reducing agent) we obtained the Mo^V trinuclear complex $[Cp^*_3Mo_3(\mu_3\text{-}O)(\mu\text{-}O)_3(\mu\text{-}O_2CCF_3)_3]^+$ (**II**) as a salt of the $Zn_2(O_2CCF_3)_6^{2-}$ dianion.[17] The formation of these compounds demonstrates that the removal of water ligands (from the expected protonation of oxo ligands, following the reduction process) generates vacant positions that are filled by the anions of the acids used. In previous contributions,[11,18] we have mentioned that another product may also be crystallized from the reaction mixture obtained by reduction in the presence of CF_3COOH, depending on the solvent and conditions used for the crystallization. This is another triangular cluster to which the formula $[Cp^*_3Mo_3(\mu\text{-}OH)_x(\mu\text{-}O)_{6-x}]^{2+}$ was assigned on the basis of an X-ray structural analysis. However, this product could

[a] Celal Bayar University, Faculty of Sciences & Liberal Arts, Department of Chemistry,
45030, Muradiye-Manisa, Turkey
[b] Laboratoire de Chimie de Coordination, UPR CNRS 8241,
205 Route de Narbonne, 31077 Toulouse Cedex, France
Fax: +33-561-553-003
E-mail: poli@lcc-toulouse.fr

not be properly characterized because of severe disorder problems in the cation as well as in the CF_3COO^- anion. This situation did not even allow the unambiguous identification of the *x* value (number of hydrogen atoms on the bridging oxygen atoms), and thus of the number of electrons in the cluster. We have now repeated the same reaction with a related strong acid, CF_3SO_3H, and crystallized the corresponding product. We report here the structure of these compounds and a description of their properties.

Results

Structure of the Trifluoroacetate Salt

The general procedure for the reduction of $[Cp^*_2Mo_2O_5]$, i.e. zinc reduction in a water-methanol solution acidified by CF_3COOH, has been described previously.[19] Numerous subsequent syntheses and crystallization of the resulting product consistently gave the same kind of crystals, which were always affected by the initially observed severe disorder problem (see above).[20] Interestingly, the same product (as revealed by the EPR study, vide infra) was also obtained in the presence of other weaker acids, in an attempt to obtain other kinds of carboxylate derivatives analogous to the previously reported $[Cp^*_2Mo_2(\mu\text{-}O)_2(\mu\text{-}O_2CCH_3)_2]$, when working at the same low pH.[16] This observation attests to the thermodynamic stability of this product.

Although badly disordered, the structure of the trifluoroacetate salt serves to identify the structural motif and to set the stage for the discussion of this compound. A view of the central Mo_3O_6 core, including the interaction with the two CF_3CO_2 anions, is shown in Figure 1 (a). The three Mo atoms form a nearly ideal equilateral triangle (vide infra), each edge of which is symmetrically bridged by two oxygen atoms, with one above and one below the Mo_3 plane. Thus, the three O atoms above the metal plane, and the three below, define two additional approximately equilateral triangles that are parallel to, and staggered with respect to, the Mo_3 triangle. The two anions are located above and below the Mo_3 plane and establish hydrogen-bonding interactions with the bridging O atoms, which desymmetrize the triangle. Both bridging O atoms of one particular Mo_3 edge (namely Mo1–Mo2 in Figure 1, a) are engaged in hydrogen bonding, each with an O atom of a different trifluoroacetate anion. The second O atom of each CF_3COO^- anion interacts with a bridging O atom of a different edge (O4 bridges Mo1–Mo3 and O6 bridges Mo2–Mo3). The four O···O distances, in the range 2.59–2.64 Å, unambiguously show the presence of four OH groups. However, the quality of the structure is not sufficient to establish whether the two remaining bridging O atoms carry additional H atoms or not. Although of low quality, the structure of the trifluoroacetate salt indicates that the unique Mo1–Mo2 distance is slightly longer (2.797 Å) than the other two (Mo1–Mo3 2.786 Å; Mo2–Mo3 2.785 Å). It is important to stress that the spectroscopic and magnetic properties are insufficient to make an unambiguous choice because both an $(OH)_4(O)_2$ and a $(OH)_6$ structure correspond to an odd number of electrons (paramagnetic). Thus, they would not be easily distinguishable by EPR spectroscopy. They are likewise difficult to distinguish by infrared spectroscopy.

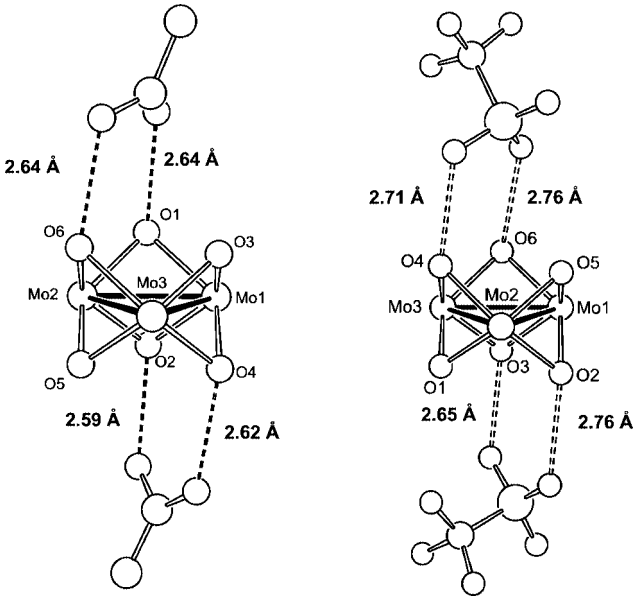

Figure 1. An ORTEP view of the central Mo_3O_6 core of $[Cp^*_3Mo_3(\mu\text{-}O)_2(\mu\text{-}OH)_4]^{2+}$ in the acetate (left, the disordered F atoms are not shown) and trifluoromethanesulfonate salts (right), showing the hydrogen-bonding interactions with the two anions.

Structure of the Trifluoromethanesulfonate Salt

The reduction process described in the previous section was repeated in the presence of triflic acid, with two objectives in mind. First, the different anion may allow a less problematic crystal-structure determination. Second, and most important, the triflate anion has three equivalent oxygen atoms available for hydrogen bonding. Therefore, should the two additional bridging functions that are not involved in hydrogen bonding with the trifluoroacetate anions (i.e. O3 and O5 in Figure 1, a) also bear hydrogen atoms, the triflate ions would be expected to establish an interaction with them. Conversely, the lack of such interactions may be taken as a strong indication against the presence of H atoms in these positions.

Complex $[Cp^*_3Mo_3(\mu\text{-}O)_2(\mu\text{-}OH)_4](CF_3SO_3)_2$ crystallizes under the same experimental conditions that lead to the crystallization of its trifluoroacetate congener. The compound dissolves readily in chlorinated solvents (dichloromethane, chloroform) and has identical EPR properties to those of the trifluoroacetate salt (vide infra). It is important to note that the crude product also gave NMR resonances that could be attributed to the Cp* protons of one or more diamagnetic products. However, a sample of carefully cleaned single crystals from the batch used for the X-ray structural analysis yielded NMR-silent $CDCl_3$ solutions.

The single-crystal X-ray analysis gave an orthorhombic unit cell and the structure was solved in the *Pbca* space

group. A peculiar twinning problem prevented refinement of the data to very low residuals (see Experimental Section). However, the structure was apparently not complicated by interstitial solvent, nor by disorder. The strongest residual peak and hole in the last difference Fourier map were reasonably low and without any chemical significance. A view of the $[Cp^*_3Mo_3(\mu\text{-}O)_2(\mu\text{-}OH)_4]^{2+}$ cation is shown in Figure 2.

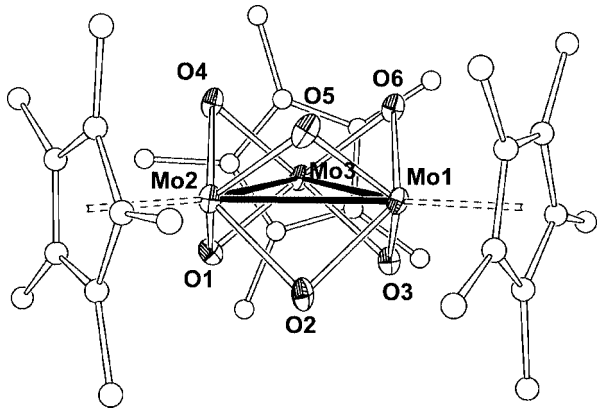

Figure 2. An ORTEP view of the $[Cp^*_3Mo_3(\mu\text{-}O)_2(\mu\text{-}OH)_4]^{2+}$ ion from the structure of the trifluoromethanesulfonate salt. For clarity, the hydrogen atoms of the Cp* ligands are not shown and the ellipsoids of the Cp* C atoms are replaced by spheres of arbitrary radius. The ellipsoids of the Mo and O atoms are shown at the 30% probability level.

The relative arrangement of the ions in the structure is shown in Figure 1 (b). Like in the related trifluoroacetate salt, only two of the three bridging groups on each triangular face establish hydrogen bonds with the oxygen atoms of the CF_3SO_3 anions. The third O atom of each trifluoromethanesulfonate anion does not point toward the third bridging O atom. Specifically, the CF_3SO_3 anion located on the same side occupied by the bridging O1, O2, and O3 atoms places the third SO_3 oxygen atom away from (*exo*), and the CF_3 group on the same side as (*endo*), the triangle of the bridging O atoms. One CF_3 fluorine atom is in proximity of atom O1, but the F···O distance (3.22 Å) is too long to envisage a hydrogen bond (sum of van der Waals radii of F and O: 2.75 Å). The second CF_3SO_3 anion, which is located on the same side as O4, O5 and O6 from the Mo_3 triangle, places the third O atom *endo* and the CF_3 group *exo*, but the anion is tilted in such a way as to place the third O atom at 4.02 Å from O5, clearly indicating a repulsive interaction (sum of van der Waals radii of the two O atoms: 2.80 Å). This evidence allows us to propose the molecular formula of the dicationic trimetallic cluster as having four bridging hydroxo and two bridging oxo groups. Although the structure of the trifluoroacetate salt (vide supra) is much less precisely determined than that of the trifluoromethanesulfonate salt, a comparison of the hydrogen bonded O···O contacts shows that these are tighter with the former anion and looser with the latter one, in agreement with their relative basicity.

Although the structure has no crystallographically imposed symmetry, the trimetallic dication possesses an approximate C_2 local symmetry, with the pseudo-symmetry axis passing through the Mo2 atom and the middle of the Mo1–Mo3 bond. We shall refer to all averaged bonding parameters by using the symbol Mo for the unique atom Mo2 and the symbol Mo′ for the two pseudo-symmetry related Mo1 and Mo3 atoms. The unique Mo′–Mo′ bond is marginally, but significantly, longer than the two Mo–Mo′ bonds, possibly as a consequence of the different nature of the bridging groups. Indeed, the bridging Mo–(μ-O) and Mo′–(μ-O) bonds are significantly shorter than the corresponding Mo–(μ-OH) and Mo′–(μ-OH) bonds. The alternative interpretation of assigning a greater oxidation state (+5) to the Mo atom and a lower one (+4) to the Mo′ atoms seems excluded by the density functional calculations (vide infra). There is no significant difference, neither between the Mo–(μ-O) and Mo′–(μ-O) bonds [average 1.95(1) Å] nor between the Mo–(μ-OH) and Mo′–(μ-OH) bonds [average 2.05(1) Å], in agreement with an insignificant difference in metal ionic radius between Mo and Mo′. This analysis further serves to confirm the interpretation of atoms O1 and O5 as (μ-O) rather than (μ-OH) groups. The Mo–Mo distances are slightly longer than those found in related triangular $[Cp^*_3Mo_3(\mu\text{-}O)_6]$-type clusters, e.g. 2.730(13) Å in $[Cp^*_4Mo_5O_{11}]$ (where the central $[Cp^*_3Mo_3(\mu\text{-}O)_6]^-$ unit is capped by a $[Cp^*Mo^{VI}O_2(\mu\text{-}O)Mo^{VI}O_2]^+$ fragment),[21] and 2.744(9) Å in $[Cp^*_6Mo_8O_{16}]$ (where two equivalent $[Cp^*_3Mo_3(\mu\text{-}O)_6]^-$ units are bridged by a $[Mo^V_2O_2(\mu\text{-}O)_2]^{2+}$ fragment).[22] They are identical, on the other hand, to the average distance reported for $[Cp^*_3Mo_3(\mu\text{-}OH)_n(\mu\text{-}O)_{6-n}]Cl_2$ [2.78(3) Å]. The latter structure, however, was poorly defined because of solvent disorder.[21]

Mass Spectrometric Characterization

Both salts (trifluoroacetate and triflate) were investigated by electrospray mass spectrometry (positive mode) in mixed H_2O/MeOH solvents. In both cases the spectrum shows the presence of trinuclear species and the absence of mono- and dinuclear species. For the trifluoroacetate salt, the major envelope is satisfactorily simulated on the basis of the formula $[Cp^*_3Mo_3(\mu\text{-}O)_5(\mu\text{-}OMe)]^+$ (see Figure 3). This shows that, under the conditions of the electrospray MS experiment, the dication readily loses one proton and exchanges the residual bridging OH group with the methanol solvent. The shape of the simulated envelope matches very closely the experimental one, but the major peak *m*/*z* value leaves a doubt as to the exact number of protons. This question was resolved by the additional experiments that will be presented in later sections. The minor envelope (Figure 3, c) corresponds to the formula ($[Cp^*_3Mo_3(\mu\text{–}O)_5(\mu\text{-}OMe)]^+$ + CF_3COOH + MeOH) and therefore gives direct evidence for the presence of the trifluoroacetate anion. This envelope overlaps with a weaker peak distribution at higher *m*/*z* values, which could correspond to further addition of a water molecule. A parallel FAB (NBA matrix) spectrometric analysis shows the absence of solvent association phenom-

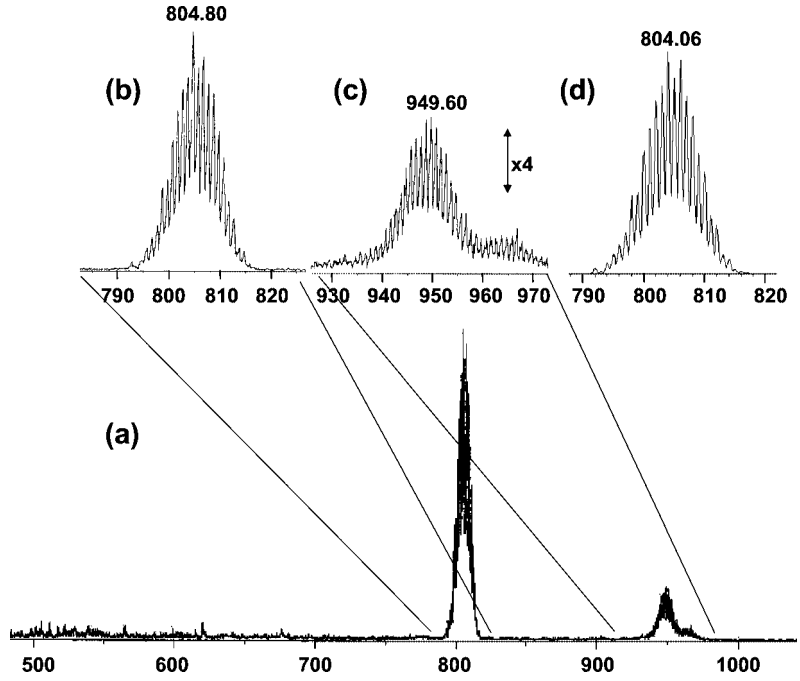

Figure 3. (a) Electrospray mass spectrum (positive mode) of $[Cp^*_3Mo_3(\mu\text{-}O)_4(\mu\text{-}OH)_2](O_2CF_3)_2$ in MeOH. Portions of this spectrum are shown in (b) and (c), and a simulation of the envelope corresponding to the $[Cp^*_3Mo_3(\mu\text{-}O)_5(\mu\text{-}OMe)]^+$ ion is given in (d).

ena. However, the spectrum is more complex because of reduction and fragmentation of the trinuclear unit. The highest peak distributions observed correspond to $[Cp^*_3Mo_3O_4(OH)_2]$ (massif centered around m/z = 791) and $[Cp^*_3Mo_3O_4(OH)]$ (massif centered around m/z = 774).

The spectrum of the triflate salt is closely related to that of the trifluoroacetate analogue. The major envelope, centered around m/z = 804, is identical to that observed for the trifluoroacetate analogue (the major peak is found at m/z = 804.25 in this case), whereas the smaller envelope at higher m/z values is centered at 1036.35, corresponding to $([Cp^*_3Mo_3(\mu\text{-}O)_5(\mu\text{-}OMe)]^+ + CF_3SO_3H + 2\,MeOH + H_2O)$. Thus, this mass spectrum also gives direct evidence for the presence of the triflate counterion.

EPR Spectroscopic Properties

Solutions of the complex $[Cp^*_3Mo_3(\mu\text{-}O)_2(\mu\text{-}OH)_4]^{2+}$ (either salt) in dichloromethane exhibit a relatively sharp EPR spectrum at room temperature (see Figure 4), whereas the compounds are NMR-silent in $CDCl_3$. The absence of an NMR spectrum is consistent with the odd-electron nature of the cluster. The observation of an isotropic EPR spectrum at relatively high temperature, on the other hand, clearly indicates that the system must have a single unpaired electron (S = ½) in a nondegenerate orbital. An accurate analysis of the Mo hyperfine coupling pattern helps us determine the localization of the unpaired electron. As Figure 4 shows, simulations were carried out using hyperfine coupling constant, shape, and line-broadening parameters from the experimental spectrum, but assuming coupling to either one, two, or all three cluster Mo atoms. The height and shape of the satellite peaks, relative to the central resonance and especially relative to each other, unambiguously identify the spectrum as involving coupling to two equivalent Mo nuclei. Unfortunately, the relative broadness of the spectrum conceals the outer peaks of the 1:2:3:4:5:6:5:4:3:2:1 envelope (6.25% overall intensity), which is generated by the isotopomers having two I = 5/2 Mo nuclei. The spectrum was also recorded at temperatures down to 210 K in an attempt to improve the spectral resolution, but no significant change was noted.

Magnetic Susceptibility

The compound exhibits a simple Curie behavior consistent with the presence of a single unpaired electron. Measurements carried out in the 6–60 K range show a linear χ^{-1} vs. T plot, with a negligible value for the Curie temperature (–0.38 K; see Figure 5).

The corresponding effective magnetic moment, which is approximately temperature independent, averages 1.66 μ_B after correction for the ligands' diamagnetism. This is rather close to the expected spin-only value for one unpaired electron (1.73 μ_B). This result is consistent with the EPR spectrum and confirms that the latter is representative of the bulk sample.

Density Funtional Calculations

In order to further confirm the assignment of the chemical composition and electronic structure, we carried out a theoretical study. Before describing the computational results, it is useful to qualitatively analyze the electronic struc-

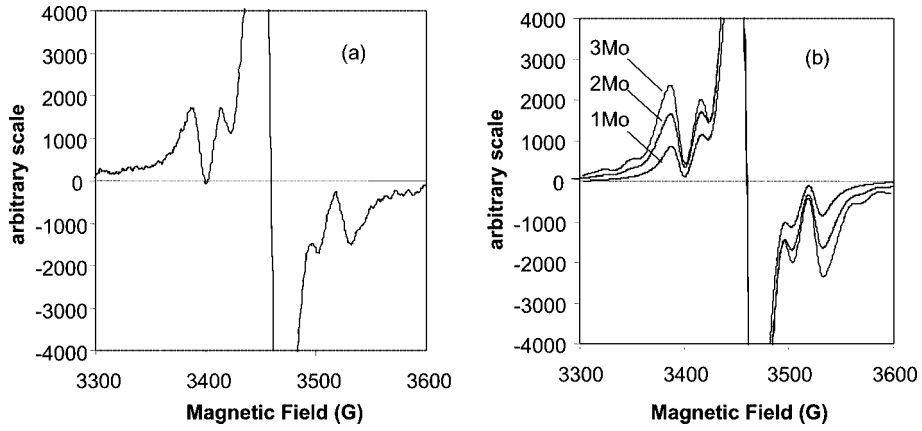

Figure 4. EPR spectrum of $[Cp^*_3Mo_3(\mu\text{-}O)_2(\mu\text{-}OH)_4](CF_3SO_3)_2$ in CH_2Cl_2 solution. (a) Experimental spectrum. (b) Simulated spectra with coupling to one, two, and three equivalent Mo nuclei (simulation parameters: Gaussian line shape, linewidth: 18 G). All spectra are scaled to the same peak-to-peak height for the central resonance.

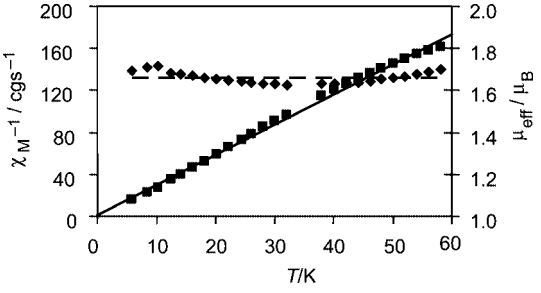

Figure 5. Magnetic properties (molar magnetic susceptibility, χ_M, and effective magnetic moment, μ_{eff}) of $[Cp^*_3Mo_3(\mu\text{-}O)_2(\mu\text{-}OH)_4](CF_3SO_3)_2$.

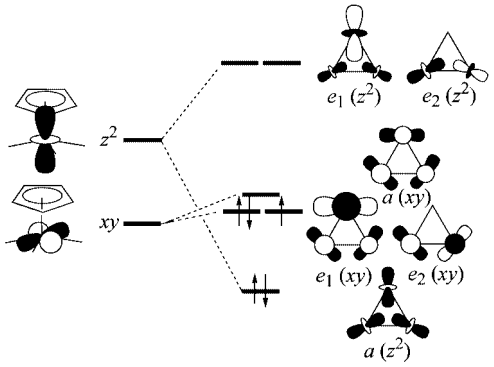

Scheme 1.

ture on the basis of first principles and relevant previous knowledge.[21,23,24] The cluster may be viewed as resulting from the assembly of three "four-legged piano stools" of the Cp^*MoO_4 type, whose electronic structure is well known,[25,26] as shown in Scheme 1. Taking a D_{3h}-symmetrical structure with six identical bridging ligands as a first approximation, it is possible to envisage that the interaction of the z^2-type orbitals will lead to one bonding (of type *a*) and two degenerate antibonding (of type *e*) combinations, and that the interaction of the *xy*-type orbitals will equally lead to one *a*-type bonding and two degenerate antibonding *e*-type combinations. As the overlap between the *xy* orbitals is much weaker, the energy of the MOs resulting from these orbitals will be less perturbed from that of the starting fragment orbitals. However, as well documented for other bridging systems, π* mixing with the bridging ligands' lone pairs should destabilize the *xy* orbital combinations.[27] It is easily predictable that this destabilization should be strongest for the symmetric (*a*-type) orbital, as shown in Scheme 1. The asymmetric nature of the bridging ligands (four OH and two O), however, is expected to alter this scheme, particularly by removing the degeneracy of the *e*-type combinations.

The DFT-optimized geometry agrees quite well with the experimental geometry (see Table 1). The minor variations could partly be attributed to the different environment (hydrogen-bonded, solid-state structure with the CF_3SO_3 anion for the experimental geometry, free, "gas-phase" dication for the DFT-optimized one); and partly to the well-known overestimation of bond lengths by DFT. In particular, it is comforting to see the same trend of Mo–O bond lengths [Mo-(μ-O) < Mo-(μ-OH)] in the optimized and experimental parameters, once again confirming the structural assignment.

The calculated electronic structure (Figure 6) confirms the qualitative expectations. The bonding $a(z^2)$ orbital is located just above the group of the six MOs describing the three double-sided Mo–Cp* π interactions. Above it, we find the pair of $e(xy)$ orbitals, which contains three electrons. The calculation converges with two electrons in the e_1-type orbital and one in the e_2-type orbital, whose degeneracy (in the ideal C_3 symmetry) is substantially split by the different nature of the bridging groups (O vs. OH). It is rewarding to see that the unpaired electron, according to the calculations, chooses to reside in the orbital from the *e* set that has the nodal plane parallel to the C_2 symmetry axis (e_2), rather than in the orbital with the nodal plane perpendicular to it (e_1). The half-occupied orbital has contributions only from the two Mo′ atoms and a symmetry-imposed zero contribution from the Mo atom, in perfect

Table 1. Selected bond lengths [Å] and angles [°] for $[Cp^*_3Mo_3(\mu\text{-}O)_2(\mu\text{-}OH)_4]^{2+}$: observed (from the X-ray structure of the CF_3SO_3 salt) and DFT-optimized (gas-phase).

Distance[a,b]	Experimental	DFT-optimized
Mo–Mo′	2.7854(13), 2.7820(13)	2.859, 2.876
Mo′–Mo′	2.8244(12)	2.946
Mo–(μ-O)	1.946(8), 1.959(8)	1.979, 1.987
Mo–(μ-OH)	2.041(8), 2.061(7)	2.108, 2.110
Mo′–(μ-O)	1.949(8), 1.956(8)	1.938, 1.943
Mo′–(μ-OH)	2.048(8), 2.053(7), 2.055(8)	2.090, 2.094, 2.097
	2.049(8), 2.028(8), 2.053(8)	2.099, 2.106, 2.108
Mo–CNT	2.0145(9)	2.082
Mo′–CNT	2.0058(9), 2.0168(9)	2.079, 2.080

Angle[a,b]	Experimental	DFT-optimized
Mo′–Mo–Mo′	60.97(3)	61.92
Mo–Mo′–Mo′	59.46(3), 59.57(3)	58.91, 59.16
Mo–(μ-O)–Mo′	91.0(3), 90.9(3)	93.61, 93.83
Mo–(μ-OH)–Mo′	85.1(3), 85.9(3)	85.96, 85.97
Mo′–(μ-OH)–Mo′	87.5(3), 87.0(3)	88.93, 88.94
CNT–Mo–(μ-O)	112.7 (2), 114.7(2)	114.04, 116.94
CNT–Mo–(μ-OH)	112.2(2), 112.7(2)	113.22, 113.92
CNT–Mo′–(μ-O)	113.4(2), 113.9(2)	113.01, 113.92
CNT–Mo′–(μ-OH)	110.8(2), 113.4(2), 115.1(2)	112.94, 115.54, 117.05
	111.7(2), 114.8(2), 115.0(2)	112.99, 115.30, 117.88

[a] Mo indicates the unique atom with a $[Cp^*Mo(O)_2(OH)_2]$ coordination environment and Mo′ indicates the two symmetry-related atoms with a $[Cp^*Mo(O)(OH)_3]$ coordination environment. [b] CNT indicates the ring centroid of the pentamethylcyclopentadienyl ligand.

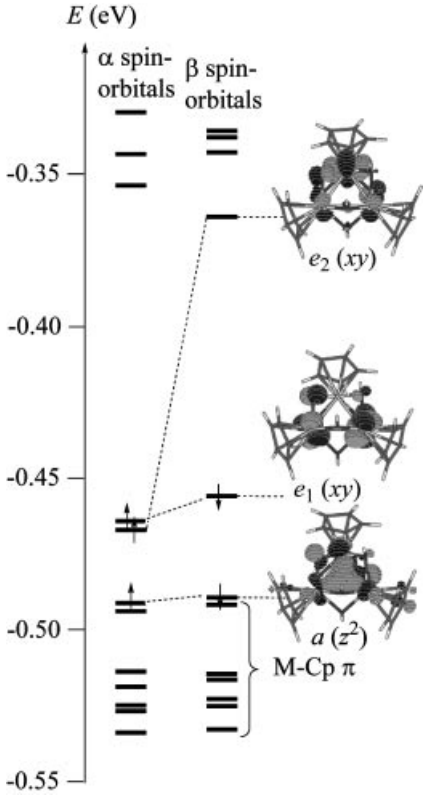

Figure 6. Electronic structure of the $[Cp^*_3Mo_3(\mu\text{-}O)_2(\mu\text{-}OH)_4]^{2+}$ cluster as resulting from a gas-phase DFT calculation. The shape of the spin-orbitals connected by a dashed line is essentially identical (only one for each pair is shown).

agreement with the result of the EPR analysis above. Furthermore, the DFT calculation suggests that the cluster is completely valence-delocalized. Indeed, the computed natural charge[28] is very similar on atoms Mo (+1.075) and Mo′ (+1.100 and 1.101), and so is the computed Mulliken spin density (–0.820, 0.849, and 0.847, respectively). We note that the mean value of S^2 from the spin-unrestricted calculation is high (see Computational Details), suggesting the mixing of an excited $[a(z^2)]^2[e_1(xy)]^1[a_2(xy)]^1[a(xy)]^1$ configuration into the ground state. However, according to the result of the EPR experiment, this contribution must be negligible for the real system because the isotropic resonance is relatively sharp at room temperature and unaffected by cooling.

A somewhat related triangular Mo_3 cluster, $[Mo_3CuS_4(H_2O)_{10}]^{4+}$, which was described as having a Cu^I ion and a Mo_3^{11+} core,[29] has an electronic structure similar to that described here, although there are two additional electrons, thereby also involving occupation of the *a*(xy)-type orbitals. In that case, the experimental observation of electronic coupling to a single Mo nucleus in the EPR spectrum was interpreted as resulting from a valence-trapped $Mo^{IV}Mo^{IV}Mo^{III}$ structure, the unpaired electron being mostly localized on the Mo^{III} center, although the calculations (at the EHMO level) indicated a delocalized shape for the MOs similar to that reported here.

Discussion

It is useful to compare the salts reported here with a closely related one reported by Bottomley et al., namely $[Cp^*_3Mo_3(\mu\text{-}O)_{6-n}(\mu\text{-}OH)_n]^{2+}(Cl^-)_2$.[21] This compound was obtained by a synthetic strategy closely related to ours (zinc reduction of $[Cp^*MoO_2Cl]$ in $CHCl_3$ in the presence of concentrated HCl). The X-ray structure presented for this compound was affected by severe disorder, thus preventing the unambiguous determination of the number of bridging OH groups, as for the trifluoroacetate complex reported here. We have already pointed out above that the reported Mo–Mo distances for the dichloride salt are very similar to those reported here for the $[Cp^*_3Mo_3(\mu\text{-}O)_2(\mu\text{-}OH)_4]^{2+}$-$(CF_3SO_3^-)_2$ salt. For $[Cp^*_3Mo_3(\mu\text{-}O)_{6-n}(\mu\text{-}OH)_n]^{2+}(Cl^-)_2$, the authors proposed 5 as the most likely *n* value, but also suggested the presence of a redox disproportionation equilibrium in solution that involves other species characterized by *n* = 4 and *n* = 6. This suggestion was based on magnetic, EPR, and NMR observations. In particular, the EPR spectrum was assigned to the *n* = 6 species, whereas two NMR resonances − a sharp one and a broad one − were assigned to the diamagnetic *n* = 5 species and to the paramagnetic *n* = 4 species, respectively. The room-temperature isotropic EPR spectrum reported for solutions of the dichloride salt seems very similar to that of the trifluoromethanesulfonate

and trifluoroacetate salts reported here, but it was interpreted in that case as arising from coupling to three equivalent Mo nuclei. An argument given in favor of the above scheme is the fact that the $n = 4$ species could not yield an observable isotropic EPR spectrum, given the expected $(e)^3$ electronic configuration.[21] Our DFT calculation, however, shows that the asymmetry associated with the distribution of the two μ-O and four μ-OH groups splits this orbital degeneracy significantly. The trifluoromethanesulfonate and trifluoroacetate salts reported here (at least batches of clean single crystals) do not show any sharp or even broadened NMR signal that could be assigned to the Cp* ligand in a diamagnetic or paramagnetic compound. All evidence, therefore, points to the fact that the trifluoromethanesulfonate salt reported here maintains its identity as a single compound in solution.

Another useful comparison involves compounds $[Cp^*_4Mo_5O_{11}]$[21] and $[Cp^*_6Mo_8O_{16}]$,[22] both of which are described as containing a central $[Cp^*_3Mo_3(\mu\text{-}O)_6]^-$ unit (vide supra). In this unit, there are only four cluster electrons ($Mo_3^{IV,V,V}$) and the structures are stabilized by capping one triangular O_3 face with either Mo^V or Mo^{VI} ions. Therefore, it seems possible that the salts of $[Cp^*_3Mo_3(\mu\text{-}O)_2(\mu\text{-}OH)_4]^{2+}$ exhibit interesting electrochemical properties, which may be dependent on pH and/or on the presence of other metal ions.

Conclusion

We have shown in this paper that the zinc reduction of $[Cp^*_2Mo_2O_5]$ in an acidic aqueous environment leads to the triangular $[Cp^*_3Mo_3(\mu\text{-}O)_2(\mu\text{-}OH)_4]^{2+}$ cluster, containing a paramagnetic (five-electron) trimetallic core. The spectroscopic evidence points to a solution structure identical to the solid-state structure, with the unpaired electron located in a delocalized molecular orbital that has atomic orbital participation from only two Mo atoms. A study of the redox properties and acid/base properties of this system, followed by an investigation of its chemical reactivity, are now in progress and will be reported in due course.

Experimental Section

General Methods: All preparations and manipulations were carried out with Schlenk techniques under an oxygen-free argon atmosphere. All glassware was oven-dried at 120 °C. Solvents were dried by standard procedures and distilled under dinitrogen prior to use. EPR spectra were measured with an Elexsys E500 Bruker spectrometer (X-band) equipped with both a frequency meter and a gaussmeter. Magnetic susceptibility measurements were carried out with a MPMS5 QUANTUM DESIGN magnetometer. Mass spectra were recorded with a NERMAG R10-10 instrument. The starting compound $[Cp^*_2Mo_2O_5]$ was prepared as described in the literature.[19]

Synthesis and Crystallization of $[Cp^*_3Mo_3(\mu\text{-}O)_2(\mu\text{-}OH)_4](CF_3SO_3)_2$: Metallic zinc (20 mesh, 0.48 g, 7.38 mmol) was added to a solution of $[Cp^*_2Mo_2O_5]$ (0.05 g, 0.092 mmol) in MeOH/H_2O (1:1, 6 mL) after acidification with concentrated CF_3SO_3H (10 drops). The mixture was stirred under argon at room temperature for two days, during which time it changed from a clear, yellow solution to a green suspension. The mixture was filtered and the solid was dried in vacuo. The solid was extracted with THF and, after filtration, addition of *n*-hexane yielded a green precipitate (0.021 g, 31.3%). A single crystal for the X-ray analysis was obtained by diffusion of *n*-hexane into a green CH_2Cl_2 solution at room temperature.

$C_{32}H_{49}F_6Mo_3O_{12}S_2{\cdot}2CH_2Cl_2$ (1261.53): calcd. C 32.37, H 4.23; found C 32.92, H 3.65. EPR (CH_2Cl_2): $g = 1.962$, $a_{Mo} = 26.2$ G. Average μ_{eff} in the 6–60 K range: 1.66 μ_B (diamagnetic correction: -7.91×10^{-4} cgs).

X-ray Analyses: Single crystals of $[Cp^*_3Mo_3(\mu\text{-}O)_2(\mu\text{-}OH)_4](X)_2$ (X = CF_3CO_2, CF_3SO_3) were mounted under inert perfluoropolyether at the tip of a glass fiber and cooled in the cryostream of an Oxford-Diffraction XCALIBUR CCD diffractometer. Data were collected using monochromatic Mo-K_α radiation ($\lambda = 0.71073$). The structures were solved by direct methods (SIR97[30]) and refined by least-squares procedures on F^2 using SHELXL-97.[31] Although the model could be easily defined by direct methods for both structures, its refinement appeared to be very poor, with large elongated ellipsoids for the Cp* and rather high R and wR_2 values. The CF_3CO_2 salt did not lead to a successful refinement, so this structure is not further commented. For the CF_3SO_3 salt, the elongated ellipsoids suggest a free rotation of the Cp ring around the Mo–Cp* centroid axis. However, all attempts to refine a disordered Cp* model failed. The occurrence of a twinned structure by pseudo merohedry, considering a monoclinic cell, was also attempted but again without improvement of the refinement. Refinement in a noncentrosymmetric space group did not improve the result either. Careful examination of the reciprocal space revealed that the crystal used was certainly not single but an attempt to integrate using different domains failed. There is, however, no doubt about the reality of the model, as confirmed by different analytical methods. All H atoms attached to carbon were introduced in the calculation in idealized positions and treated as riding models. Owing to the poor quality of the refinement, the H atom attached to the hydroxy groups could not be located. The drawings were produced with the help of ORTEP32.[32] The structures were solved by direct methods (SIR97)[30] and refined by least-squares procedures on F^2 using SHELXL-97.[31] All H atoms attached to carbon were introduced in calculation in idealized positions and treated as riding models. The drawing of the molecules was realized with the help of ORTEP32.[32] The crystal data and refinement parameters are shown in Table 2 and selected geometric parameters are collected in Table 1.

Computational Details: The DFT calculation was carried out on a model system where the Cp* ligands were replaced by the simpler Cp rings. The starting geometry was based on the crystallographically determined structure of the triflate salt and no symmetry restrictions were imposed. The geometry was fully optimized and the resulting minimum of the potential energy surface (PES) was verified by the positive value of all second derivatives of the energy. The calculation, which used the spin-unrestricted formulation, was performed using the B3LYP three-parameter hybrid density functional method of Becke,[33] as implemented in the Gaussian03 suite of programs.[34] The basis sets used for the geometry optimizations are the standard 6-31G** for C, H, and P atoms, and the standard LANL2DZ basis set, which includes the Hay and Wadt effective core potentials (ECP),[35] for the metal atoms. The value of $<S^2>$ resulting from the calculation is 1.39 (0.81 after annihilation). This shows that there is significant spin contamination, indicating mixing with low-lying excited states. The correspondence between the resulting Kohn–Sham spin-orbitals was verified by producing contour plots with the aid of the program MOLDEN.[36]

Table 2. Crystal data and refinement parameters for $[Cp^*_3Mo_3(\mu\text{-}O)_2(\mu\text{-}OH)_4](CF_3SO_3)_2$.

Empirical formula	$C_{32}H_{35}F_6Mo_3O_{12}S_2$
Formula weight	1087.62
Temperature	180(2) K
Wavelength	0.71073 Å
Crystal system	orthorhombic
Space group	*Pbca*
Unit-cell dimensions	a = 15.5156(6) Å
	b = 16.8899(7) Å
	c = 31.0271(12) Å
	α = 90°
	β = 90°
	γ = 90°
Volume	8130.9(6) Å^3
Z	8
Density (calculated)	1.777 Mg m^{-3}
Absorption coefficient	1.098 mm^{-1}
F(000)	4360
Crystal size	0.24 × 0.12 × 0.077 mm^3
Theta range for data collection	2.82 to 26.37°
Index ranges	$-19 \le h \le 19$
	$-18 \le k \le 21$
	$-38 \le l \le 38$
Reflections collected	59030
Independent reflections	8302 [R(int) = 0.0997]
Completeness to θ = 26.37°	99.8%
Absorption correction	Semi-empirical from equivalents
Max. and min. transmission	0.9623 and 0.7409
Refinement method	Full-matrix least-squares on F^2
Data / restraints / parameters	8302 / 0 / 487
Goodness-of-fit on F^2	1.088
Final R indices [$I > 2\sigma(I)$]	R_1 = 0.1145, wR_2 = 0.2423
R indices (all data)	R_1 = 0.1279, wR_2 = 0.2495
Largest diff. peak and hole	2.867 and –3.776 e Å^{-3}

Acknowledgments

This research was supported by the CNRS in France and by TUBITAK in Turkey. Supplemental travel support by a bilateral CNRS-TUBITAK (TBAG-U/62-102T211) program is also gratefully acknowledged. In addition, R.P. acknowledges support from the European Commission through the Research Training Network "AQUACHEM" (contract No. MRTN-CT-2003-503864), the COST D29 program (working group 0009-03) and CINES for a grant of free computing time. F.D. thanks the University of Celal Bayar (FEF, 2002/101) for a research grant. We thank Alain Mari for assistance with the EPR and magnetic susceptibility measurements and analyses.

[1] T. Chan, L. Li, Y. Yang, W. Lu, *ACS Symp. Ser.* **2002**, *819*, 166–177.
[2] F. Joó, *Acc. Chem. Res.* **2002**, *35*, 738–745.
[3] I. T. Horvath, *Acc. Chem. Res.* **2002**, *35*, 685.
[4] D. Sinou, *Topic in Current Chemistry* **1999**, *206*, 41–59.
[5] D. Sinou, *Adv. Synth. Catal.* **2002**, *344*, 221–237.
[6] P. Kalck, F. Monteil, *Adv. Organomet. Chem.* **1992**, *34*, 219–284.
[7] B. E. Hanson, *Coord. Chem. Rev.* **1999**, *186*, 795–807.
[8] C. Muller, D. Vos, P. Jutzi, *J. Organomet. Chem.* **2000**, *600*, 127–143.
[9] W. A. Herrmann, E. Herdtweck, M. Flöel, J. Kulpe, U. Küsthardt, J. Okuda, *Polyhedron* **1987**, *6*, 1165–1182.
[10] W. A. Herrmann, *Comments Inorg. Chem.* **1988**, *7*, 73–107.
[11] R. Poli, *Chem. Eur. J.* **2004**, *10*, 332–341.
[12] E. Collange, J. Garcia, R. Poli, *New J. Chem.* **2002**, *26*, 1249–1256.
[13] J. Gun, A. Modestov, O. Lev, D. Saurenz, M. A. Vorotyntsev, R. Poli, *Eur. J. Inorg. Chem.* **2003**, 482–492.
[14] J. Gun, A. Modestov, O. Lev, R. Poli, *Eur. J. Inorg. Chem.* **2003**, 2264–2272.
[15] E. Collange, L. Metteau, P. Richard, R. Poli, *Polyhedron* **2004**, *23*, 2605–2610.
[16] F. Demirhan, P. Richard, R. Poli, *Inorg. Chim. Acta* **2003**, *347*, 61–66.
[17] F. Demirhan, J. Gun, O. Lev, A. Modestov, R. Poli, P. Richard, *J. Chem. Soc., Dalton Trans.* **2002**, 2109–2111.
[18] E. Collange, F. Demirhan, J. Gun, O. Lev, A. Modestov, R. Poli, P. Richard, D. Saurenz, in *Perspectives in Organometallic Chemistry* (Eds.: C. G. Screttas, B. R. Steele), Royal Society of Chemistry, London, **2003**, vol. 287, pp. 167–182.
[19] D. Saurenz, F. Demirhan, P. Richard, R. Poli, H. Sitzmann, *Eur. J. Inorg. Chem.* **2002**, 1415–1424.
[20] Crystal data for compound $[Cp^*_3Mo_3(\mu\text{-}O)_2(\mu\text{-}OH)_4](CF_3CO_2)_2$: monoclinic, $P2_1/c$, a = 15.537(2) Å, 15.195(1) Å, 16.763(2) Å, β = 94.46(1)..
[21] F. Bottomley, J. Chen, K. F. Preston, R. C. Thompson, *J. Am. Chem. Soc.* **1994**, *116*, 7989–7995.
[22] J. R. Harper, A. L. Rheingold, *J. Am. Chem. Soc.* **1990**, *112*, 4037–4038.
[23] P. Hofmann, N. Roesch, H. R. Schmidt, *Inorg. Chem.* **1986**, *25*, 4470–4478.
[24] F. Bottomley, S. Karslioglu, *Organometallics* **1992**, *11*, 326–337.
[25] P. Kubácek, R. Hoffmann, Z. Havlas, *Organometallics* **1982**, *1*, 180–188.
[26] T. A. Albright, J. K. Burdett, M. H. Whangbo, *Orbital Interactions in Chemistry*, John Wiley & Sons, New York, **1985**.
[27] F. Abugideiri, J. C. Fettinger, R. Poli, *Inorg. Chim. Acta* **1995**, *229*, 445–454.
[28] A. E. Reed, L. A. Curtiss, F. Weinhold, *Chem. Rev.* **1988**, *88*, 899–926.
[29] R. Miyamoto, S. Kawata, M. Iwaizumi, H. Akashi, T. Shibahara, *Inorg. Chem.* **1997**, *36*, 542–546.
[30] A. Altomare, M. Burla, M. Camalli, G. Cascarano, C. Giacovazzo, A. Guagliardi, A. Moliterni, G. Polidori, R. Spagna, *J. Appl. Crystallogr.* **1999**, *32*, 115–119.
[31] G. M. Sheldrick, *SHELXL97. Program for Crystal Structure refinement*, University of Göttingen, Germany, **1997**.
[32] L. J. Farrugia, *J. Appl. Crystallogr.* **1997**, *30*, 565.
[33] A. D. Becke, *J. Chem. Phys.* **1993**, *98*, 5648–5652.
[34] M. J. Frisch, G. W. Trucks, H. B. Schlegel, G. E. Scuseria, M. A. Robb, J. R. Cheeseman, J. Montgomery, J. A., T. Vreven, K. N. Kudin, J. C. Burant, J. M. Millam, S. S. Iyengar, J. Tomasi, V. Barone, B. Mennucci, M. Cossi, G. Scalmani, N. Rega, G. A. Petersson, H. Nakatsuji, M. Hada, M. Ehara, K. Toyota, R. Fukuda, J. Hasegawa, M. Ishida, T. Nakajima, Y. Honda, O. Kitao, H. Nakai, M. Klene, X. Li, J. E. Knox, H. P. Hratchian, J. B. Cross, C. Adamo, J. Jaramillo, R. Gomperts, R. E. Stratmann, O. Yazyev, A. J. Austin, R. Cammi, C. Pomelli, J. W. Ochterski, P. Y. Ayala, K. Morokuma, G. A. Voth, P. Salvador, J. J. Dannenberg, V. G. Zakrzewski, S. Dapprich, A. D. Daniels, M. C. Strain, O. Farkas, D. K. Malick, A. D. Rabuck, K. Raghavachari, J. B. Foresman, J. V. Ortiz, Q. Cui, A. G. Baboul, S. Clifford, J. Cioslowski, B. B. Stefanov, G. Liu, A. Liashenko, P. Piskorz, I. Komaromi, R. L. Martin, D. J. Fox, T. Keith, M. A. Al-Laham, C. Y. Peng, A. Nanayakkara, M. Challacombe, P. M. W. Gill, B. Johnson, W. Chen, M. W. Wong, C. Gonzalez, J. A. Pople, *Gaussian 03, Revision B.04*, Gaussian, Inc., Pittsburgh PA, **2003**.
[35] P. J. Hay, W. R. Wadt, *J. Chem. Phys.* **1985**, *82*, 270–283.
[36] G. Schaftenaar, *Molden v3.2*, CAOS/CAMM Center Nijmegen, Toernooiveld, Nijmegen, The Netherlands, **1991**.

Received: July 25, 2005
Published Online: December 22, 2005

